

A Multi-sensors System for Human Motion Measurement: Preliminary Setup

M. Harshe*

INRIA

Sophia-Antipolis, France

J-P. Merlet[†]

INRIA

Sophia-Antipolis, France

D. Daney[‡]

INRIA

Sophia-Antipolis, France

S. Bennour[§]

ENIM

Monastir, Tunisia

Abstract— *Gait analysis and human joint motion measurement has been studied extensively in the recent past. Common approaches that have been used include using inertial sensors, multi-camera optical and IR tracking systems, X-ray and fluoroscopy based imaging, force sensors, magnetic sensors and bone-fixed pins for measurement. Soft tissue artifacts (STA) are a common source of error in most type of measurements and the standard procedure in gait analysis has been to use a combination of measurement methods for efficient estimation of joint angles and the link poses. However, there are few studies where a multiple number of methods have been compared and the correlation between results from various approaches studied. In this paper, we propose an outline for measurement for human joint motion using a number of sensors that can give complete information relating to the joints.*

Our proposed experiment assumes a human joint to be a 6 DOF joint between 2 links. We will mount collars on the limbs close to anatomical landmarks, treating the actual pose of the system with respect to the bones as unknowns. These collars will hold markers and sensors that will be used in the experiments. We will be using a 10 camera optical (IR) tracking system, accelerometers and gyroscopes, 7 wire passive measurement system, 7 wire active measurement system, in-shoe pressure pads, variable length resistive wires, collar-mounted force sensors, and IR distance sensor to measure the pose of the trunk. Our experiment will focus on the knee joint and it's motion during activities such as walking. This paper describes the experimental setup and the sensor and collar calibration that has been performed.

Keywords: Cable-based parallel manipulators, Gait analysis, inertial sensors, knee kinematics

I. Introduction

The human gait analysis has been the subject of various studies. [1] provides an exhaustive review of clinical gait analysis, viewed through the kinematic perspective. The motion of the tibio-femoral joint has been investigated often, and a review of its motion is discussed in [2]. The techniques employed for motion analysis have been quite varied. Studies have compared the use of intra-cortical pin

based markers against skin-based markers [3], [4], [5], [6], [7], [8] in determining human bone motion. Intra-cortical pin based markers provide data with least possible errors, however the process is quite invasive and cannot be replicated on a majority of patients.

Magnetic Resonance (MR), X-ray, CT imaging methods have been used for capturing pose data and calculating joint angles [9], [10], [11]. These methods are limited to static experiments and provide an incomplete picture about human joint behavior [12]. Some studies using dynamic MRI for real-time and in vivo experiments [13] note the high cost of the MRI scanners needed. Fluoroscopy imaging and optical motion capture systems have been used to obtain 3 dimensional motion data [14], [15], [16], [17] and also assess the STA [18], [19].

A widely used approach is to attach inertial sensors to the patient limbs as has been done by [20], [21], [22], [23], [24], [25]. The efficiency of attachment systems has also been investigated by [26] and accelerometer orientation and error compensation methods have been proposed by [27]. These studies suggest that inertial sensors provide a relatively inexpensive way to observe knee motion. Other studies have employed parallel mechanisms for modeling and measuring human joint motion [28], [29], [30], [31].

While these studies provide a good picture about knee joint motion, few have investigated the comparison of all possible approaches. Most studies have used one or two methods and have compared the results. In this paper we describe our proposed experiment that will employ at least seven different types of sensors and measurement techniques to analyze human gait. Our experiment is proposed to measure the motion of the human knee, but the method described can be extended to measure motions of other joints.

The experimental setup and the approach for measuring motion is described in Section II. The sensors, and equipment that will be used for the experiment is described in Section III along with a description of the issues encountered and resolved. The collar fixed to the thigh is the most important piece of hardware built for the experiment. All measurements of the experiments depend on the performance of the collar. Hence a separate section, Section IV, is devoted to describing the collar construction and its calibration.

*Mandar.Harshe@inria.fr

[†]Jean-Pierre.Merlet@inria.fr[‡]David.Daney@inria.fr[§]Sami.Bennour@enim.rnu.tn

II. Experimental Setup

Our approach to measuring joint motion, which in our case will be the knee joint, will be to implement a multitude of surface based sensors attached using collars. Two adjustable collars will be fixed on the thigh and the tibial shank each of the patient (see Fig. 1). The collars are made up plates connected by hinges (Fig. 2), and one adjustable elastic strap to account for variations in the patients' physical characteristics. The elastic strap is also needed to ensure that the collar is held firmly against the skin. The reflective markers for optical motion capture system, the accelerometers, connection points for passive and active wire systems, and the force sensors are located on these collars. We will also have an IR distance sensor array to measure the pose of the trunk. A model of the set-up showing the passive wire measurement system connected to the tibia, the frame of the MARIONET robot and a treadmill is shown in Fig. 3. The actual experimental set-up, using only sensors mounted on the collars on tibia, is shown in Fig. 4.

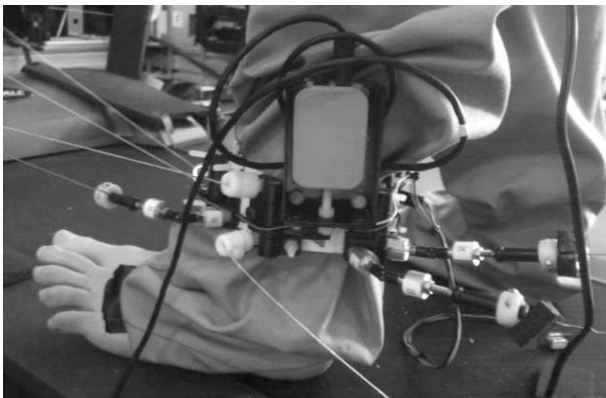


Fig. 1. A collar fixed on the tibial shank, holding an accelerometer. Wires from active and passive wire measurement systems are also connected



Fig. 2. Actual collar components: Plates with 4 reference points, connected by a hinge. The tips of the 4 screws are the 4 reference points

The location of collars with respect to the bone depends on patient anatomy and the variations. The collars will be fixed close to anatomical landmarks and these distances will be measured. However, STA imply that during walking and running the location of collars, and hence the markers, will change. This change in location (and orientation)

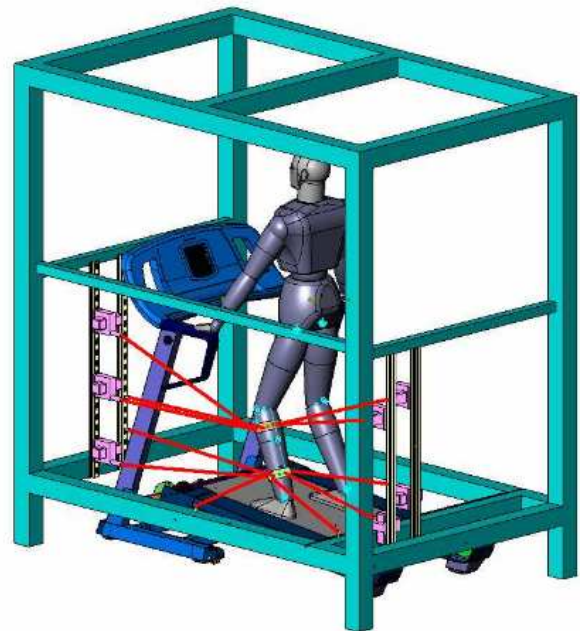


Fig. 3. A 3D model of the experimental set-up: The outer frame is the frame of the MARIONET robot. The wires of the passive measurement system are shown

lies within some bounds. We will model this location of collar with respect to the bone as unknowns to be solved for. Variable length resistive wires between the collars on thigh and tibia will be used to keep track of the spatial relation between the collars. Since each collar will hold at least one of each type of sensor, our aim is to over-determine the system. This will provide us a way to completely quantify the motion taking into account the data from all sensors. The data obtained can be used for comparative analysis and error checking.

Force sensors mounted on the insides of the collars will provide the data relating to muscle activity during motion. In-shoe force sensors will provide information describing the pressure variation across the foot over each step cycle. The active wire system can be used for corrective forces in the later stages of the experiments, where motion of the joint may be restricted.

Our proposed experiments involves observing the motion of the knee joint during standard human activities. It is also important to determine the range of motions that a normal human knee undergoes. We intend to record motions during exercises such as walking on a treadmill, rowing, balancing and sit to stand motion.

III. Materials

The 7 wire-driven parallel robot, MARIONET, developed at INRIA [32] and a 7 wire passive measurement system (POSIWIRE WS17KT, ASM, Germany) treat the collars and the human leg as the end-effector of a parallel robot. The inertial sensors (MTx, Xsens Technologies B.V,

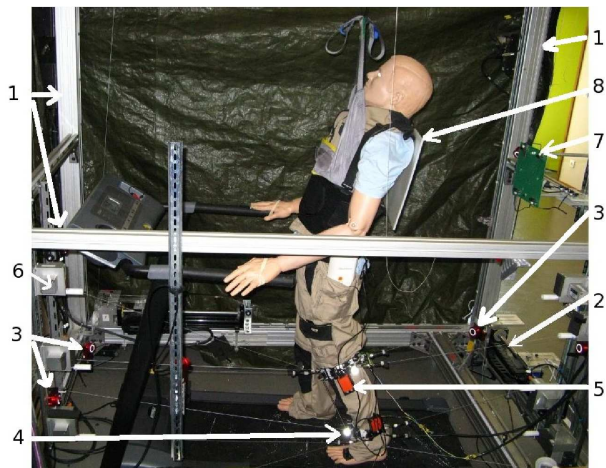


Fig. 4. The experimental set-up: (1) Frame of the MARIONET robot (2) Actuators for the MARIONET (3) Cameras for optical motion capture (4) Reflective markers for optical motion capture (5) Accelerometers (6) Passive wire measurement system (7) IR distance sensor array (8) Reflective board for IR sensor array

Netherlands) are mounted on each collar to measure the 3-D acceleration, angular velocity and orientation vectors [25] of the plate it is attached to. A 10 camera motion capture system (Optitrack Full Body Motion Capture, NaturalPoint Inc, USA) is used to capture the motion of markers mounted on the collars. In-shoe pressure pads (F-Scan Mobile, Tekscan, USA) will be used to record weight distribution variation. Force sensors (FlexiForce, Tekscan, USA) mounted on the insides of the collar measure the variation of the muscle pressure on the collar. IR sensors (1103 IR Reflective sensor, Phidgets Inc, Canada) are fixed facing the back of the patient in order to measure the pose of the trunk.

A. MARIONET wire-driven robot

The MARIONET is a seven wire parallel robot designed for modularity. The collar and human leg is treated as an end-effector of the system. The wires are connected to linear actuator (Copley Motion type M 2506) through a pulley system. The motion of actuator platform is measured by a linear incremental encoder with an accuracy of $1 \mu\text{m}$ [32].

B. Passive wire measurement

The sensors used are the cable actuated position sensors with a measuring range for 0 to 2500 mm. The cables are stainless steel and the precision potentiometer gives an analog voltage output between 0 to 10V, essentially giving it an infinite resolution. Phidgets adapters are used, with LabVIEW software, to record data from the sensors.

C. Inertial Sensors: Xsens Motion Capture

The Xsens MTx sensors are miniature inertial 3DOF orientation trackers that provide drift-free data. These sensors record raw data and have in-built algorithms to calculate

calibrated output specifying the 3D orientation, acceleration, rate of turn and earth magnetic field. The sensors are set to record synchronously and the data collected is transmitted over wireless Bluetooth link to a workstation.

C.1 Reference Frames

Each sensor is set to provide the acceleration (in m/s^2) and angular velocity (deg/s) with respect to body-fixed reference frame and the orientation with respect to ground reference plane (defined as local north, west, up for x,y,z axis respectively). The orientation data is represented using quaternions as it provides information using the least memory space and avoids Euler angle singularities.

The accelerometers measure all accelerations experienced by the sensor, including acceleration due to gravity. Hence, to calculate the free acceleration, we must subtract the gravitational effects. The acceleration output given by the sensor is the acceleration experienced by the physical sensor inside the casing, expressed in the body-fixed coordinate system. The orientation data is to be used to represent the quantities in a global/ground reference frame.

C.2 Timestamps

The device measures the UTC time at the moment the sensor takes in measurements. This UTC time is in milliseconds and is needed in order to correlate accelerometer data with data obtained from other sensors.

C.3 Sensor Numbering

The XBus Master, which interconnects and synchronizes the sensors, detects the total number of sensors automatically and numbers the sensors according to decreasing device-Id numbers.

D. NaturalPoint Optitrack

The Optitrack Full Body Motion capture system by NaturalPoint includes a 12 camera system, along with proprietary software (Arena Motion Capture). We use 10 of these cameras, mounted on the MARIONET robot frame to record the complete motion of the leg. The 10 cameras ensure that the reflective markers fixed to the collars are always visible to at least 3 cameras. The software is equipped with a calibration wizard that ensures accurate marker position data.

D.1 Output Data and Timestamping

The proprietary software provided along with the camera gives the data in C3D file format, which stores marker data with respect to the frame number. The camera system are designed to provide a fixed frame rate (in this case 100 fps). The data is not timestamped and hence, an “event”, which can be measured by the other systems that determine UTC times, is needed to assign approximate UTC time to the frames.

E. In-shoe Pressure pads

The Tekscan F-Scan Mobile system is an untethered plantar pressure/force measurement system. The sensors are placed under the feet, inside the patients' shoes, and the data is recorded on the receiver unit. This receiver unit is normally strapped to the patient's body and stores the pressure data until the unit is connected to a computer via USB. The system can export the sensed pressures and the coordinates of the center of force for each frame into an ASCII file.

F. Collar Force Pads

Force sensors are mounted on the insides of each component plate of the collar. These sensors will record the variation of pressure on the collar due to muscle activity. The sensors are covered with foam padding to prevent accidental damage. Fig. 5 shows two adjacent plates showing the actual set up.

The sensors are 0.2mm thick with a 9.5mm diameter sensing area. The FlexiForce sensors use a resistive-based technology. The application of a force to the active sensing area of the sensor results in a change in the resistance of the sensing element in inverse proportion to the force applied.

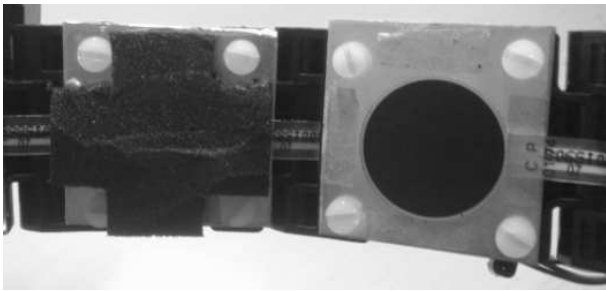


Fig. 5. Inside of the collar with force sensors. The right plate is shown with the foam padding removed.

G. IR reflective sensors

An array of IR sensors is mounted on a frame so that it points towards the patients' back. The sensors detect the presence of an object and provide an output sensor value that varies with distance between the object and the sensor. A planar reflective pad is fixed to a vest that will be worn by the patient. The array of sensors will detect the location of reflective pad. Since the shape of the pad is known, the output of the sensors can be used to calculate the pose of the reflective pad. This will enable us to calculate the pose of the trunk.

IV. Collars

A. Collar Labeling

The plates have been labeled according to the position they were first installed in. The modular design permits easy re-arrangement of the plates, with respect to the

molded front plate. In our particular case, plates are labeled in the following sense:

- The front plate is labeled `frnt_crst`
- First letter denotes whether the plate is on the lower or higher collar
 - ‘h’ denotes higher collar
 - ‘b’ denotes lower collar
- Second letter denotes whether the collar is fixed to the tibia or the femur
 - ‘t’ denotes collar is on the tibia
 - ‘f’ denotes collar is on the femur
- Third letter denotes the location of the plate with respect to the front plate
 - ‘g’ denotes plate is to the left of the front plate (as seen facing the collar)
 - ‘d’ denotes plate is to the right of the front plate (as seen facing the collar)
- The number denotes the distance of the plate from the front plate, for example, 1 denotes that the plate neighbors the front plate, 2 denotes that it is the second plate from the front plate and so on.

B. Construction and Geometry

The collar used to fix sensors consists of styrene plates connected by hinge joints. These hinge joints can be fixed at a constant angle to function as a rigid joint. The plates can be unscrewed from the hinges and quickly replaced. The modular design of the collar ensures that the shape and size can be changed quickly. As a result, these collars can be adapted to use not just on different patients, with differing anatomical dimensions, but also for other experiments to measure motion of other joints.

Of the collars currently developed for the tibia, the lower collar, to be attached just above the ankle (see Fig. 1) uses 5 plates, while the upper collar uses 6 plates. All plates in the tibial collar except one are rectangular planar plates with 4 screws fixed in a rectangular array. The front plate has been molded in order to resemble the front crest of the tibial bone. This ensures that there is no slipping between the collar and the tibia.

The hinge angles and the length of the flexible strap will be the only parameters of the collar that will vary with each experiment. The collars will be adjusted for each patient by adjusting the hinge angles and tightening the elastic strap. The hinge angles will be fixed in order to ensure that the collar shape does not change and to prevent random collar movements.

In our experiment, the collar will house the sensors. Since the shape of the collar will change with each experiment, the position of reference points on each plate, with respect to the first plate, will change. For each experiment with a new user, we need to determine the hinge angles in order to know the location of the reference and attachment points in the global reference frame.

C. Kinematic Model

We consider the collar to be a serial kinematic chain, where the hinge angles are the joint variables and the plates of the collar are the links of the chain. The classical way to describe the pose of the chain (for any set of hinge angles) is to use the Denavit-Hartenberg representation [33].

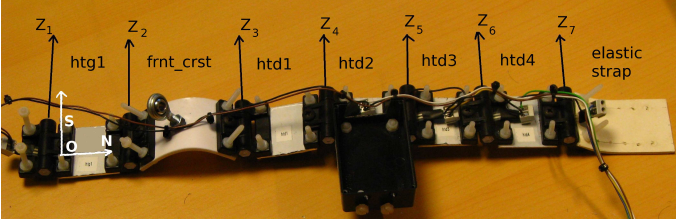


Fig. 6. Collar calibration: The hinge axis are marked as z_i . The base frame \mathcal{F} is indicated on plate `htg1` by points \mathbf{O} , \mathbf{Q} , \mathbf{R} . The assembly attached to plate `htd2` is for mounting the accelerometer.

In the DH representation, if the consecutive joint axes are parallel, the joint offset parameter is an independent variable. When the consecutive axes are not strictly parallel, the sensitivity of error in one of the DH parameters is very high. We use the method suggested in [34] and define an additional parameter. Thus, in our representation, the angles about hinge axes will be the angles about the z -axes that vary. The other four parameters - translations about z and x axis, the twist angles about x -axis and the additional rotation angle β_i about y -axis - remain constant. The reference frame defined using this method, for plate i , is denoted by \mathcal{D}_i . The transformation matrix between consecutive plate frames \mathcal{D}_{i-1} and \mathcal{D}_i is given by eq. (1).

$$\mathbf{H}_i^{i-1} = \mathbf{Rot}(y, \beta_i) \cdot \mathbf{Rot}(x, \alpha_i) \cdot \mathbf{Trans}(x, a_i) \cdot \mathbf{Rot}(z, \theta_i) \cdot \mathbf{Trans}(z, d_i) \quad (1)$$

In the closed configuration, the model of the collar having n links (plates) is given by eq. (2). Referring to Fig. 6, the axis \mathbf{Z}_i corresponds to \mathbf{H}_i^{i-1} .

$$\mathbf{I} = \mathbf{H}_2^1 \cdot \mathbf{H}_3^2 \cdot \dots \cdot \mathbf{H}_{i+1}^i \cdot \dots \cdot \mathbf{H}_1^n \quad (2)$$

Once all parameters have been identified, eq. (2) is a set of equations in the n joint angles.

The collar shown in Fig. 6 has 6 plates - 'htg1', 'frnt_crst', 'htd1' to 'htd4'. The seventh link is the flexible strap, which is taken into account during experiments. We treat 'htg1' as the base plate of the serial mechanism.

Thus, we define the following frames:

- As defined previously, let \mathcal{D}_i be the frame associated with the joint as described by the above modified DH parameters. Thus, \mathbf{H}_i^{i-1} is transformation matrix between \mathcal{D}_i and \mathcal{D}_{i-1} .
- Let \mathcal{F} be the reference frame fixed to base plate `htg1`. Referring to Fig. 6, point \mathbf{O} is considered as the origin, line

\mathbf{ON} as the x -axis, and XY plane given by the points \mathbf{ONS} . Referring Fig. 7, \mathbf{O} corresponds to \mathbf{P}_3 , \mathbf{S} corresponds to \mathbf{P}_1 and \mathbf{N} corresponds to \mathbf{P}_4 .

- Let \mathcal{L}_i be the frame fixed to plate i . Referring to Fig. 7, \mathbf{P}_1 is the origin of this coordinate system, with $\mathbf{P}_1\mathbf{P}_2$ as the x -axis and point \mathbf{P}_3 lying in the XY plane of this system.

Let \mathbf{P} be any point on plate i , and let $\mathbf{P}^{\mathcal{F}}$, \mathbf{P}^i be the coordinates of \mathbf{P} expressed in the reference frame \mathcal{F} and plate fixed DH frame \mathcal{D}_i respectively. Then we obtain the eq (3). In any configuration, \mathbf{P}^i will be a constant.

$$\mathbf{P}^{\mathcal{F}} = \mathbf{H}_2^{\mathcal{F}} \cdot \dots \cdot \mathbf{H}_1^{i-1} \cdot \mathbf{P}^i \quad (3)$$

For the particular case of the reference frame \mathcal{F} , the z -axes of the two frames are not parallel. Thus the transformation between frame \mathcal{F} and hinge frame \mathcal{D}_2 to align z -axis with the hinge axis \mathbf{Z}_2 can be expressed in terms of four fixed parameters. These resemble the standard DH parameters. Thus, $\mathbf{H}_2^{\mathcal{F}}$ is given by eq.(4), and it includes the joint rotation angle. Note that this angle θ_2 is the only parameter that is pose dependent.

$$\mathbf{H}_2^{\mathcal{F}} = \mathbf{Rot}(z, \phi) \cdot \mathbf{Trans}(z, d) \cdot \mathbf{Rot}(x, \alpha) \cdot \mathbf{Trans}(x, a) \cdot \mathbf{Rot}(z, \theta_2) \quad (4)$$

D. Calibration

In the classical calibration of serial chains, the pose of the end-effector is measured and for each pose the joint angles are noted. The DH parameters are identified using this data. We note that in our case, this classical method is not adopted. Each plate on the collar has attachment and reference points that need to be identified in the local frame. Also, the joints do not possess encoders to measure the joint angles.

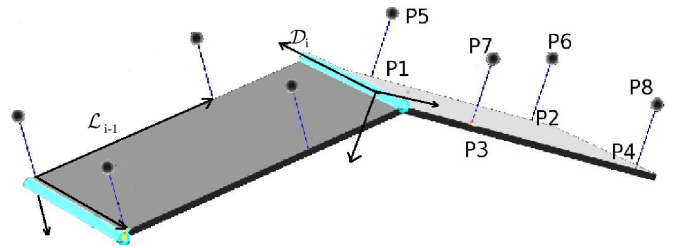


Fig. 7. Model of collar components: $\mathbf{P}_1, \mathbf{P}_2, \mathbf{P}_3, \mathbf{P}_4$ are defined at the base of the screws. Points $\mathbf{P}_5, \mathbf{P}_6, \mathbf{P}_7, \mathbf{P}_8$ are the tips of screws. Lines $\mathbf{P}_1\mathbf{P}_5, \mathbf{P}_2\mathbf{P}_6, \mathbf{P}_3\mathbf{P}_7, \mathbf{P}_4\mathbf{P}_8$ define the four screws. These 8 points are the reference points for each plate. Axes for frames \mathcal{L}_{i-1} and \mathcal{D}_i are also shown.

Hence we employ a variation of standard calibration method. We identify the plate parameters progressively, using data obtained from plate i to identify parameters for plate $i + 1$. This calibration process consists of two stages. The first stage is to identify the constant parameters of the collar that are independent of the collar pose. This stage is done before the experiment. The next stage consists of

identifying the joint angles once the collar has been fixed on a patient for an experiment. This stage of calibration is performed during the experiment.

D.1 Calibration before experiment

In this section, we describe the process of calibration that needs to be done before conducting experiments. The process is the same for any two successive links, and so we describe the steps for a generic identification process. The approach for plates 1 and 2 is slightly different and we describe it first.

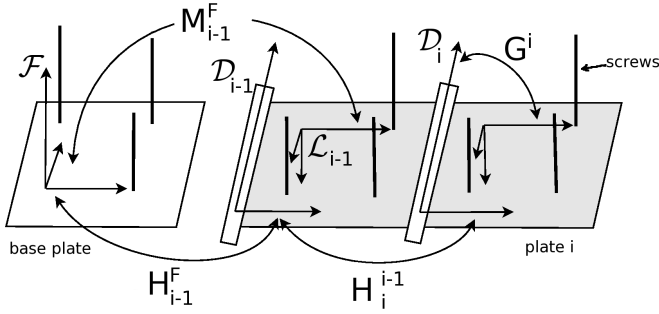


Fig. 8. Plate frames and transformation matrices. The bold lines indicate the screws. \mathcal{F} is the reference frame on the base plate $\text{htg}1$, \mathcal{D}_{i-1} and \mathcal{D}_i are indicated at the Z-axis of the respective frames.

Assume plates 1 to $i-1$ have been calibrated and the parameters have been identified, for a given pose of the $i-1$ plates. Referring to Fig. 7, in the following paragraphs, we refer to the left plate as plate $(i-1)$ and the right plate as plate i .

- Let \mathbf{G}^i be the transformation matrix between frames \mathcal{L}_i and \mathcal{D}_i .
- Let \mathbf{M}_i^F be the transformation matrix between frames \mathcal{L}_i and \mathcal{F} .

Note that \mathbf{M}_i^F can be calculated based on measurements of reference points \mathbf{P}_1 to \mathbf{P}_8 ¹. These transformation matrices can be visualized in Fig. 8. For the first two plates, we can write eq (5). Note that from eq (4), \mathbf{H}_2^F is a function of 5 variables - a, d, α, ϕ and θ .

$$\mathbf{M}_2^F = \mathbf{H}_2^F \cdot \mathbf{G}^2 \quad (5)$$

The matrix \mathbf{G}^2 can be expressed as a result of translation by vector $\mathbf{t}'_2 = [t_{2x}, t_{2y}, t_{2z}]$, and a rotation expressed in Rodrigues parameters as $\mathbf{q}_2 = [q_{2x}, q_{2y}, q_{2z}]$ define . We define ζ_2 as,

$$\zeta_2 = [a, d, \phi, \alpha, \theta, t_{2x}, t_{2y}, t_{2z}, q_{2x}, q_{2y}, q_{2z}] \quad (6)$$

Let \mathbf{X}_2 be the 6×1 vector of position and orientation (expressed using Rodrigues parameters) extracted from a homogeneous transformation matrix $\mathbf{H}_2^F \cdot \mathbf{G}^2$. This vector is

¹As described earlier, \mathbf{M}_i^F is defined such that the origin of \mathcal{L}_i is at \mathbf{P}_1 , the x-axis is along $\mathbf{P}_1\mathbf{P}_2$ and \mathbf{P}_3 lies on the XY plane.

a function of the vector ζ_2 . As \mathbf{M}_2^F can be calculated from measurements, a vector \mathbf{X}_{2m} associated with this matrix is a known quantity. For $1 \dots k$ poses assumed by plate 2, the number of unknowns in system of equations generated is $(\mathbf{k} + 10)$ (from eq (6) since we define joint angle θ for the first pose to be zero. A least squares method [35] will allow us to determine a ζ using eq (7).

$$\min_{\zeta} \|\mathbf{X}_2 - \mathbf{X}_{2m}\|^2 \quad (7)$$

The system obtained consists of $6\mathbf{k}$ equations. Hence at least 2 poses are necessary to get the best estimates for the unknowns.

For the general case for a plate, with $i \geq 3$, we can write eq (8), assuming the ideal case with no measurement errors.

$$\mathbf{M}_i^F = \mathbf{H}_{i-1}^F \cdot \mathbf{H}_i^{i-1} \cdot \mathbf{G}^i \quad (8)$$

In this case, the matrix \mathbf{G}^i is composed of a translation by vector $\mathbf{t}_i = [t_{ix}, t_{iy}, t_{iz}]$ and rotation by $\mathbf{q}_i = [q_{ix}, q_{iy}, q_{iz}]$ (expressed in Rodrigues parameters). We define ζ to be the vector of parameters in eq (10), as given in eq (9).

$$\zeta = [a_i, \beta_i, \alpha_i, \theta_i, \mathbf{t}'_i, \mathbf{q}'_i] \quad (9)$$

As we assume that plates 1 to $i-1$ have been calibrated, \mathbf{H}_{i-1}^F is already known, while \mathbf{M}_i^F is known from measurements. Thus, we can rewrite eq (8) by grouping the knowns and define an error term as eq (10).

$$\epsilon = \mathbf{H}_{i-1}^F \cdot \mathbf{M}_i^F - \mathbf{H}_i^{i-1} \cdot \mathbf{G}^i \quad (10)$$

\mathbf{X}_i be the 6×1 vector of position and orientation (expressed using Rodrigues parameters) extracted from a homogeneous transformation matrix ($\mathbf{H}_i^{i-1} \cdot \mathbf{G}^i$). This vector is a function of the vector ζ . Let vector \mathbf{X}_m be associated with $\mathbf{H}_{i-1}^F \cdot \mathbf{M}_i^F$. As noted earlier, this can be determined from known results and measurements.

For $1 \dots k$ poses assumed by plate i , the number of unknowns in system of equations generated by eq (10) is $(\mathbf{k} + 9)$. We define joint angle θ for the first pose to be zero. A least squares method will allow us to determine a ζ using eq (11).

$$\min_{\zeta} \|\mathbf{X}_i - \mathbf{X}_{im}\|^2 \quad (11)$$

This provides us with a system of $6\mathbf{k}$ equations. Hence at least 2 poses are necessary to get the best estimates for the unknowns.

D.2 Calibration during experiment

Once the constant parameters are found, the reference points for each plate can be represented in the local frames \mathcal{D}_i attached to that plate. This description of the plates is independent of collar orientation and pose. The collar has a flexible strap and when it is fixed on a patient, the only unknowns in describing the collar configuration are the hinge

angles and the length of the flexible strap. These joint angles in each experiment will be calculated based on sensor measurements, the plate parameters and the local, plate fixed co-ordinates of reference points, using equations (3) and eq (8).

This data will then be used to calculate the co-ordinates of the reference points in a global frame, thus providing data about the motion of the human leg.

V. Conclusions

Our experiment envisions using a large number of sensors to collect all possible data while tracking human motion. Multiple measurements and redundant data will ensure that we can make generalized assumptions about the joint. The joint will be treated as a 6 DOF joint, accounting for the minor translations and rotations. The large number of measurements will also permit us to treat collar location with respect to bone as variables. Thus, we will address the problem associated with STA. The force measurements and trunk pose measurements will also help up create an exhaustive set of data that can be used for further study.

References

- [1] D.H. Sutherland. The evolution of clinical gait analysis, part ii kinematics. *Gait & Posture*, 16(2):159–179, 2002.
- [2] M.A.F. Freeman and V. Pinskerova. The movement of the normal tibio-femoral joint. *J. of Biomechanics*, 38(2):197–208, 2005.
- [3] M.S. Andersen et al. Do kinematic model reduces the effect of soft tissues artifacts in skin marker-based motion analysis ? an in vivo study of knee kinematics. *J. of Biomechanics*, 43(2):268–273, 2010.
- [4] D.L. Benoit et al. Effect of skin movement artifact on knee kinematics during gait and cutting motions measured in vivo. *Gait & Posture*, 24(2):152–164, 2006.
- [5] Reinschmidt C. et al. Effect of skin movement on the analysis of skeletal knee joint motion during running. *J. of Biomechanics*, 30(7):729–732, 1997.
- [6] A. Cappozzo et al. Position and orientation in space of bones during movement: experimental artifacts. *Clinical Biomechanics*, 11(2):90–100, 1996.
- [7] A. Leardini et al. Human movement analysis using stereophotogrammetry part 3. soft tissue artifact assessment and compensation. *Gait & Posture*, 21(2):212–225, 2005.
- [8] K. Manal et al. Knee moment profiles during walking: errors due to soft tissue movement of the shank and the influence of the reference coordinate system. *Gait & Posture*, 15(1):10–17, 2002.
- [9] A. Hemmerich et al. Measuring three-dimensional knee kinematics under torsional loading. *J. of Biomechanics*, 42(2):183–186, 2009.
- [10] E.J. McWalter et al. A single measure of patellar kinematics is an inadequate surrogate marker for patterns of three-dimensional kinematics in healthy knees. *The Knee*, 17(2):135–140, 2010.
- [11] B. Innocenti et al. An in-vitro study of human knee kinematics: natural vs. replaced joint. In *4th European Conference of the International Federation for Medical and Biological Engineering*, Antwerp, 23-27 November 2008.
- [12] F. Lavoie et al. Gesture as an important factor in 3D kinematic assessment of the knee. *Knee Surgery, Sports Traumatology, Arthroscopy*, 16(1):64–70, 2008.
- [13] A.R. Seisler and F.T. Sheehan. Normative three-dimensional patellofemoral and tibiofemoral kinematics: A dynamic, in vivo study. *Biomedical Engineering, IEEE Transactions on*, 54(7):1333–1341, jul. 2007.
- [14] M. Ringer and J. Lasenby. A procedure for automatically estimating model parameters in optical motion capture. *Image and Vision Computing*, 22(10):834–850, 2004.
- [15] T-W. Lu et al. In vivo three dimensional kinematics of the normal knee during active extension under unloaded and loaded conditions using single-plane fluoroscopy. *Medical Engineering & Physics*, 30(8):1004–1012, 2008.
- [16] S. Corazza, L. Mündermann, and T. Andriacchi. A framework for the functional identification of joint centers using markerless motion capture, validation for the hip joint. *J. of Biomechanics*, 40(15):3510–3515, 2007.
- [17] A. Von Porat et al. Knee kinematics and kinetics during gait step and hop in males with a 16 years old ACL injury compared with matched controls. *Knee Surgery, Sports Traumatology, Arthroscopy*, 14(6):546–554, 2006.
- [18] A. Cappello et al. Soft tissue artifact compensation in knee kinematics by double anatomical landmark calibration: performance of a novel method during selected motor tasks. *IEEE Trans. on Biomedical Engineering*, 52(6):992–998, 2005.
- [19] M. Akbarshahi et al. Non-invasive assessment of soft-tissue artifact and its effect on knee joint kinematics during functional activity. *J. of Biomechanics*, 43(7):1293–1301, 2010.
- [20] P. Picerno, Cereatti A., and A. Cappozzo. Joint kinematics estimate using wearable inertial and magnetic sensing modules. *Gait & Posture*, 28(4):588–595, 2008.
- [21] J. Favre et al. Ambulatory measurement of 3D knee joint angle. *J. of Biomechanics*, 41(5):1029–1035, 2008.
- [22] J. Favre et al. Functional calibration procedure for 3D knee joint angle description using inertial sensor. *J. of Biomechanics*, 42(14):2330–2335, 2009.
- [23] G. Cooper et al. Inertial sensor-based knee flexion/extension angle estimation. *J. of Biomechanics*, 42(16):3678–3685, 2009.
- [24] J. Musić, R. Kamnik, and M. Munih. Model based inertial sensing of human body motion kinematics in sit-to-stand movement. *Simulation Modelling Practice and Theory*, 16(8):933–944, 2008.
- [25] K. Kawano et al. Analyzing 3D knee kinematics using accelerometers, gyroscopes and magnetometers. In *IEEE Conf. System of Systems Engineering*, pages 1–6, San Antonio, 16-18 April 2007.
- [26] I. Südhoff et al. Comparing three attachment systems used to determine knee kinematics during gait. *Gait & Posture*, 25(4):533–543, 2007.
- [27] W. T. Latt, U-X. Tan, C. Y. Shee, and W. T. Ang. Identification of accelerometer orientation errors and compensation for acceleration estimation errors. In *ICRA'09: Proceedings of the 2009 IEEE international conference on Robotics and Automation*, pages 577–582, Piscataway, NJ, USA, 2009. IEEE Press.
- [28] R. Di Gregorio and V. Parenti-Castelli. Parallel mechanisms for knee orthoses with selective recovery action. In *ARK*, pages 167–176, Ljubljana, 26-29 June 2006.
- [29] A. Ottoboni et al. Equivalent spatial mechanisms for modelling passive motion of the human knee. *J. of Biomechanics*, 40(0):S144–S144, 2007.
- [30] J.A. Saglia et al. A high-performance redundantly actuated parallel mechanism for ankle rehabilitation. *Int. J. of Robotics Research*, 28(9):1216–1227, September 2009.
- [31] N. Sancisi and V. Parenti-Castelli. A 1-dof parallel spherical wrist for the modelling of the knee passive motion. *Mechanism and Machine Theory*, 45(4):658–665, 2010.
- [32] J.-P. Merlet. Kinematics of the wire-driven parallel robot marionet using linear actuators. pages 3857–3862, may. 2008.
- [33] Carl D. Crane, III and Joseph Duffy. *Kinematic Analysis of Robot Manipulators*. Cambridge University Press, New York, NY, USA, 1998.
- [34] Samad A. Hayati. Robot arm geometric link parameter estimation. volume 22, pages 1477–1483, dec. 1983.
- [35] Z. Roth, B. Mooring, and B. Ravani. An overview of robot calibration. *Robotics and Automation, IEEE Journal of*, 3(5):377–385, oct. 1987.